Physics of the Earth and Planetary Interiors 257 (2016) 193–204

Contents lists available at ScienceDirect

Physics of the Earth and Planetary Interiors

journal homepage: www.elsevier.com/locate/pepi

Pn anisotropic tomography and mantle dynamics beneath China

Zhigang Zhou, Jianshe Lei *

Key Laboratory of Crustal Dynamics, Institute of Crustal Dynamics, CEA, Beijing 100085, China

ARTICLE INFO

Article history:
Received 24 January 2016
Received in revised form 5 June 2016
Accepted 8 June 2016
Available online 9 June 2016

Keywords:
Pn data
Velocity
Anisotropy
Uppermost mantle
Mantle dynamics
China

ABSTRACT

We present a new high-resolution Pn anisotropic tomographic model of the uppermost mantle beneath China inferred from 52,061 Pn arrival-time data manually picked from seismograms recorded at provincial seismic stations in China and temporary stations in Tibet and the Tienshan orogenic belt. Significant features well correlated with surface geology are revealed and provide new insights into the deep dynamics beneath China. Prominent high Pn velocities are visible under the stable cratonic blocks (e.g., the Tarim, Junngar, and Sichuan basins, and the Ordos block), whereas remarkable low Pn velocities are observed in the tectonically active areas (e.g., Pamir, the Tienshan orogenic belt, central Tibet and the Qilian fold belt). A distinct N-S trending low Pn velocity zone around 86°E is revealed under the rift running from the Himalayan block through the Lhasa block to the Qiangtang block, which indicates the hot material upwelling due to the breaking-off of the subducting Indian slab. Two N-S trending low Pn velocity belts with an approximate N-S Pn fast direction along the faults around the Chuan-Dian diamond block suggest that these faults may serve as channels of mantle flow from Tibet. The fast Pn direction changes from N-S in the north across 27°N to E-W in the south, which may reflect different types of mantle deformation. The anisotropy in the south could be caused by the asthenospheric flow resulted from the eastward subduction of the Indian plate down to the mantle transition zone beneath the Burma arc. Across the Talas-Fergana fault in the Tienshan orogenic belt, an obvious difference in velocity and anisotropy is revealed. To the west, high Pn velocities and an arc-shaped fast Pn direction are observed, implying the Indo-Asian collision, whereas to the east low Pn velocities and a range-parallel Pn fast direction are imaged, reflecting the northward underthrusting of the Tarim lithosphere and the southward underthrusting of the Kazakh lithosphere. In most parts of eastern China, pronounced low Pn velocities and a complex anisotropy pattern are observed, implying the re-orientation of the olivine arrangement in the thin lithosphere due to the westward subduction of the Pacific plate.

1. Introduction

The Chinese continent experienced many significant tectonic evolutions from Mesozoic to Cenozoic (e.g., Tapponnier and Molnar, 1975; England and Houseman, 1989; Yin and Harrison, 2000; Deng et al., 2004). The Indo-Asian collision and subsequent convergence caused high stress and compressional tectonic activities in western China (e.g., Tapponnier and Molnar, 1975; Molnar and Tapponnier, 1975), such as the uplifting of the Himalayan mountains, the Tibetan plateau and the Tienshan orogenic belt. In contrast, the westward subduction of the Pacific and Philippine Sea plates resulted in the extension of eastern China and intraplate volcanisms (Fig. 1), such as the Changbai and Wudalianchi volcanoes in northeastern China and the Datong volcano in the North China Craton (NCC) (Liu, 1999, 2000; Lei et al., 2013).

Many body- and surface-wave tomographic studies of China on various scales have been performed, providing constraints on the mantle dynamics of the Chinese continent (e.g., Lei and Zhao, 2005, 2007; Huang and Zhao, 2006; Zhao et al., 2009; Li and van der Hilst, 2010; Yao et al., 2010; Liang et al., 2012; Wei et al., 2012; Zhao and Tian, 2013; Lei et al., 2014; Bao et al., 2015; Huang et al., 2015). Shear-wave splitting analysis, for example, reflects an integrated seismic anisotropy from the crust to the upper mantle, thus has a low resolution in the vertical direction. In contrast, Pn anisotropy tomography can more precisely reveal lateral heterogeneities and anisotropy in the very limited depth range of the upper mantle. Therefore, to improve our knowledge on the structural heterogeneities and mantle dynamics of the Chinese continent, several Pn anisotropic tomographic models have recently been developed (e.g., Hearn et al., 2004; Liang et al., 2004; Pei et al., 2007; Wang et al., 2013). These previous models generally illustrate the structural features related to the geological tectonic units. For example, some high-velocity anomalies are

* Corresponding author.
E-mail address: jshlei_cj@hotmail.com (J. Lei).

http://dx.doi.org/10.1016/j.pepi.2016.06.005
0031-9201/

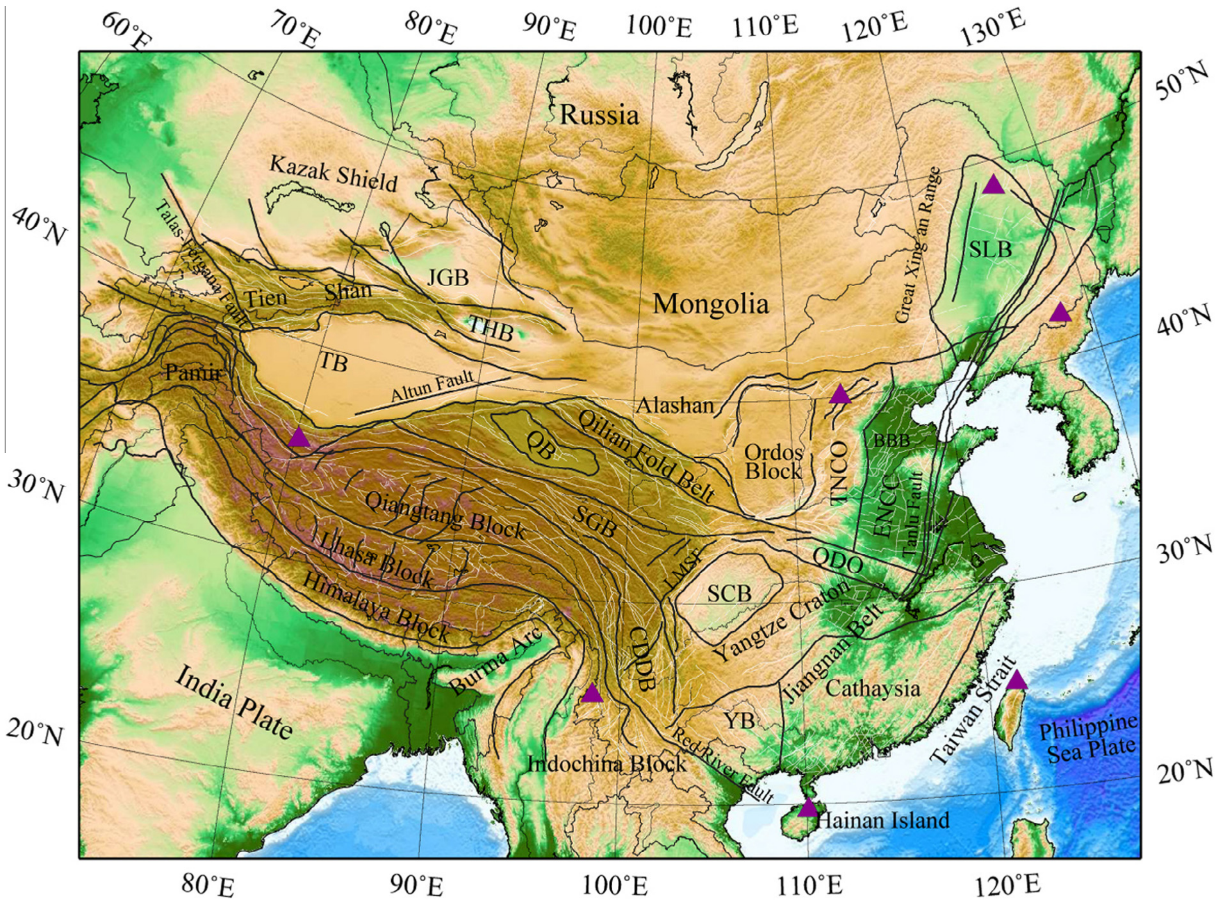

Fig. 1. Topographic map of the study region showing the main tectonic units. The thin grey lines represent the active faults (Deng et al., 2002), whereas the thick black lines denote the boundaries of tectonic blocks and major faults. The purple solid triangles denote the Cenozoic volcanoes. The abbreviations are: Junggar Basin (JGB), Tarim Basin (TB), Turpan-Hami Basin (THB), Qaidam Basin (QB), Songpan-Ganzi Block (SGB), Chuan-Dian Diamond Block (CDDB), Sichuan Basin (SCB), Youjiang Basin (YB), Trans North-China Orogen (TNCO), Eastern North China Craton (ENCC), Qinling-Dabie Orogen (QDO), Songliao Basin (SLB), Bohai Bay Basin (BBB), Longmenshan Fault (LMSF).

revealed under the Sichuan basin and Ordos block, whereas some low-velocity anomalies exist under eastern Tibet and eastern China. However, high-velocity anomalies under the Sichuan basin and Ordos block are small in lateral dimensions and low in magnitude, which cannot clearly outline the boundaries of these tectonics and significantly reflect the deep structural features under the regions. Low-velocity anomalies under eastern Tibet cannot answer if there are two obvious material flow channels in the uppermost mantle, which are revealed in the crust by recent 3-D tomographic studies (e.g., Yao et al., 2010; Bao et al., 2015). To better understand the uppermost mantle structure and dynamics of the Chinese continent, a high-quality Pn anisotropic tomographic model is required. Such a model needs a Pn data set with good accuracy and spatial coverage beyond that simply extracted from the observational bulletins. This is because the arrival times from the bulletins, such as the EHB and ABCE (the Annual Bulletin of Chinese Earthquakes), usually have large uncertainties in picking arrival times, which could result in a large damping parameter used in the inversion. In the ABCE bulletins, Pn arrival times are usually processed only for the events that occurred within the province, so many useful Pn data from smaller provinces are not collected. This may lead to insufficient ray-path coverage in certain parts of the study region.

In this study, we manually picked Pn arrival-time data from high-quality seismograms of the earthquakes with a generally uniform distribution recorded at as many portable and provincial seismic stations (Fig. 2) as possible. The waveform data are collected from the two data centres: the Data Management Centre (DMC) of the China National Seismic Network at the Institute of Geophysics, CEA (Zheng et al., 2010), and the DMC of the Incorporated Research Institutions for Seismology (IRIS). From the waveform datasets, the high-quality Pn arrival-time data are picked and inverted to obtain a high-resolution anisotropic tomographic model of the uppermost mantle beneath China. Our results shed new lights on the mantle dynamics of the Chinese continent.

2. Data

The data set used in this study comes from three sources (Fig. 2). (1) We pick 45,294 Pn arrival times from high-quality seismograms recorded at the 912 permanent seismic stations in China. To ensure the quality of seismograms, we select events ($Ms > 4.0$) from the bulletins of ABCE during 2008–2014. To reduce clustering of earthquakes, here we divide our study region into cells with a size of $0.1° \times 0.1°$ and keep the biggest earthquake in them, which leads to 1615 selected earthquakes. After our arrival-time picking, a total of 1204 earthquakes provide us with useful high-quality Pn arrival-time data. (2) Considering few provincial seismic stations in Tibet, we pick 14,696 Pn arrival times from seismograms of 944 events ($Ms > 4.0$) recorded at 386 portable seismic stations during 2003–2010. These waveform data are downloaded from the IRIS DMC website. (3) Since few arrival-time data of western Tienshan outside China are included in the ABCE, we pick 14,259 Pn data from high-quality seismograms recorded at 56 seismic stations during 1997–2001 and 2006–2011. These seismograms are